Inhibition of chondrocyte apoptosis in a rat model of osteoarthritis by exosomes derived from miR-140-5p-overexpressing human dental pulp stem cells

TIANJI LIN[1], NAN WU[2], LINHONG WANG[3], RUIPENG ZHANG[4], RUOLANG PAN[5,6] and YUN-FANG CHEN[3]

[1]Savaid Stomatology School, Hangzhou Medical College, Hangzhou, Zhejiang 310053; [2]Hospital of Integrated Traditional Chinese and Western Medicine, Hangzhou, Zhejiang 310011; [3]Department of Stomatology, Zhejiang Provincial People's Hospital, People's Hospital of Hangzhou Medical College, Hangzhou, Zhejiang 310014; [4]School of Stomatology, Zhejiang Chinese Medicine University, Hangzhou, Zhejiang 310053; [5]Key Laboratory of Cell-Based Drug and Applied Technology Development in Zhejiang Province, Hangzhou, Zhejiang 310052; [6]Institute for Cell-Based Drug Development of Zhejiang Province, S-Evans Biosciences, Hangzhou, Zhejiang 311121, P.R. China

Received August 13, 2020; Accepted December 8, 2020

DOI: 10.3892/ijmm.2020.4840

Abstract. Osteoarthritis (OA) is a common joint disorder, and the restoration of the impaired cartilage remains a main concern for researchers and clinicians. MicroRNAs (miRNAs or miRs) play crucial roles in the pathogenesis of OA. The present study examined the therapeutic efficacy of exosomal-miR-140-5p for the treatment of OA using dental pulp stem cells (DPSCs). The findings indicated that the exosomal burden of miR-140-5p was substantially increased following the transfection of DPSCs with miR-140-5p mimic. The administration of DPSC-derived exosomes promoted chondrocyte-related mRNA expression, including aggrecan, Col2α1 and Sox9, in interleukin (IL)-1β-treated human chondrocytes. This effect was substantially enhanced by miR-140-5p-enriched exosomes. The results further revealed that miR-140-5p-enriched exosomes induced a more significant reduction in IL-1β-induced chondrocyte apoptosis than the DPSC-derived exosomes. Mechanistically, it was found that miR-140-enriched DPSC-derived exosomes exerted anti-apoptotic effects, probably by regulating the expression levels of apoptosis-related proteins. Furthermore, multiple administrations of miR-140-5p-enriched exosomes substantially improved knee joint conditions in a rat model of OA. Collectively, the data of the present study suggest that exosomes derived from genetically modified DPSCs may prove to be a potential strategy for the treatment of OA.

Correspondence to: Dr Yun-Fang Chen, Department of Stomatology, Zhejiang Provincial People's Hospital, People's Hospital of Hangzhou Medical College, 158 Shangtang Road, Hangzhou, Zhejiang 310014, P.R. China
E-mail: hzcyfang1@163.com

Dr Ruolang Pan, Institute for Cell-Based Drug Development of Zhejiang Province, S-Evans Biosciences, 1500 Wenyi West Road, Hangzhou, Zhejiang 311121, P.R. China
E-mail: ruolang_pan@163.com

Key words: osteoarthritis, microRNAs, exosomal-miR-140-5p, dental pulp stem cells, apoptosis

Introduction

As determined in the mid-eighteenth century, articular cartilage, once destroyed, cannot be repaired due to the minimal regeneration capacity of articular cartilage. Small defects or injuries may cause severe pain and joint disability owing to secondary osteoarthritis (OA) (1-4). Numerous surgical techniques have been developed over the past 2 centuries, which may help to partly alleviate symptoms; however, these cannot regenerate tissue similar to native articular cartilage (5-7). One strategy is to repair tissue with properties identical to native cartilage, which integrates with the tissue to encircle the lesion. An alternative approach would be to improve the self-regeneration of articular cartilage using cells and/or other biomaterials. For this strategy, autologous mesenchymal stromal/stem cells (MSCs) have become an excellent choice. MSCs are plastic-adherent fibroblast-like cells that can be isolated from an array of mesenchymal tissues, including bone marrow, adipose tissues, umbilical cord, placenta and dental pulp (8-12). They can also differentiate into adipocytes, osteoblasts, myocytes and chondrocytes both *in vivo* and *in vitro* (13-17).

In recent years, accumulating evidence has suggested that MSCs can migrate to injured sites and affect the local microenvironment by secreting different bioactive factors, including interleukin (IL)-6, IL-10, hepatocyte growth factor, transforming growth factor-β, matrix metalloproteinases and tissue inhibitors of metalloproteinases (18-24). Moreover, the paracrine effects of MSCs are mediated by the secretion of extracellular vesicles (EVs) (13,25,26). Exosomes are a subtype of EVs, approximately 30-100 nm in diameter,

containing a particular set of protein families from intracellular compartments (27,28). MSC-derived exosomes have been investigated in different disease models and have exhibited therapeutic potential in managing stroke, Parkinson's disease and OA (29-33). MicroRNAs (miRNAs or miRs), including miR-222, miR-140 and miR-381, regulate chondrogenesis and cartilage degeneration (34-36). Previous studies have demonstrated that miR-140 plays essential roles in regulating cartilage homeostasis and development by enhancing the expression of Sox9 and aggrecan (ACAN) (37-39). Therefore, the role of miR-140 in the repair of cartilage injury in a model of OA is worthy of investigation. In the present study, miR-140-5p in was overexpressed in dental pulp stem cells (DPSCs) and an improved version of exosomes was produced from these cells, which promoted the recovery of articular cartilage injuries (Fig. S1).

Materials and methods

Human DPSC isolation and culture. Human DPSCs were provided by S-Evans Biosciences. The Ethics Committee of S-Evans Biosciences approved the collection of the human samples (no. 2020-01). Briefly, regular human third molars were extracted from adult donors (age, 18-28 years) during orthodontic treatment or due to impaction after obtaining written informed consent. Subsequently, the pulp tissue was lightly harvested and then digested in a collagenase type I (2 mg/ml) and dispase (4 mg/ml) solution for 1 h at 37˚C. After passing through a 70-μm strainer (Falcon, BD Biosciences), the cell suspension was seeded into tissue culture plates at a density of $1x10^5$/well with the α modification of Eagle's medium (Gibco; Thermo Fisher Scientific, Inc.), supplemented with 15% fetal bovine serum (FBS, Gibco; Thermo Fisher Scientific, Inc.), 2 mM l-glutamine, 100 units/ml penicillin and 100 μg/ml streptomycin. The plates were then incubated at 37˚C in 5% CO_2 using a humidified incubator and passaged by 0.25% trypsin-ethylenediaminetetraacetic acid (EDTA, Gibco; Thermo Fisher Scientific, Inc.) digestion at a 1:5 ratio.

Characterization of DPSCs and flow cytometric analysis. Osteogenic, adipogenic and chondrogenic inductions were conducted *in vitro*, as previously described, to evaluate the multilineage differentiation capacity of the DPSCs (40). To evaluate mineralization, the cultures were stained with Alizarin Red S according to the manufacturer' instructions (Cyagen Biosciences, Inc.). Briefly, cells were fixed with 4% paraformaldehyde (Beyotime Institute of Biotechnology) for 30 min and then stained with Alizarin Red S for 5 min at room temperature. Lipid droplets formed following adipogenesis induction were visualized using Oil Red O staining according to the manufacturer' instructions (Cyagen Biosciences, Inc.). Briefly, cells were fixed with 4% paraformaldehyde for 30 min followed by Oil Red O staining for 30 min at room temperature. Successful chondrogenic differentiation was tested with the use of Alcian blue staining according to the manufacturer' instructions (Cyagen Biosciences, Inc.). Briefly, cells were fixed with 4% paraformaldehyde for 30 min followed by Alcian blue staining for 30 min at room temperature.

The phenotype of the DPSCs was examined at the third passage by flow cytometry (BD FACSVerse) using antibodies, including anti-CD14 (BD Biosciences, cat. no. 555397, at a dilution of 1:5 and incubation at room temperature for 15 min), anti-CD34 (BD Biosciences, cat. no. 555822, at a dilution of 1:5 and incubation at room temperature for 15 min), anti-CD73 (BioLegend, cat. no. 344004, at a dilution of 1:20 and incubation at room temperature for 15 min), anti-CD105 (BioGems, cat. no. 17111-60, at a dilution of 1:20 and incubation at room temperature for 15 min), anti-HLA-DR (BD Biosciences, Cat. no. 555811, at a dilution of 1:5 and incubation at room temperature for 15 min) and anti-CD90 (BioLegend, cat. no. 328110, at a dilution of 1:5 and incubation at room temperature for 15 min) according to the manufacturer' instructions. The suitable isotype-matched antibody (PE; BD Biosciences, cat. no. 555749; FITC, BD Biosciences, cat. no. 555573, at dilution of 1:5 and incubation at room temperature for 15 min) was utilized as a negative control. The data were analyzed using BD FACSuite software (1.0.5.3841).

Isolation and identification of exosomes. Exosome isolation was performed using ultracentrifugation as previously described (41). In brief, culture supernatants of DPSCs were centrifuged at 3,000 x g for 30 min and then at 10,000 x g for a further 30 min at room temperature. Finally, exosomes were pelleted following centrifugation at 64,000 x g for 110 min at 4˚C using an SW28 rotor (Beckman Coulter, Inc.) and washed once with 0.32 M sucrose. Nanosight 2000 analysis and transmission electron microscopy (FEI) were utilized for the identification of exosomes that were resuspended in phosphate-buffered saline.

Cell transfection. DPSCs at the third passage were transfected with miR-140-5p mimic (20 μg/ml) or negative control (20 μg/ml) (Guangzhou RiboBio Co., Ltd.). The Amaxa Nucleofection system was adopted according to the instructions of the manufacturer of the Human Mesenchymal Stem Cell Nucleofector TM kit (Lonza Group, Ltd.). Briefly, DNA and cells were mixed in the Amaxa cuvette (Lonza Group, Ltd.) and placed in the nucleofector device. Nucleofection was conducted using the U-23 program (Lonza Group, Ltd.), which was optimized and performed as recommended by the manufacturer. Subsequently, the cuvette was rinsed with culture medium and the cells were transfer into the dish for further culture.

RNA extraction and reverse transcription-quantitative polymerase chain reaction (RT-qPCR). Total RNA was extracted using the Total Exosome RNA and Protein Isolation kit (Invitrogen; Thermo Fisher Scientific, Inc., cat. no. 4478545) according to the manufacturer's protocol, and the amount of RNA isolated was quantified using a NanoDrop spectrophotometer (NANO-100; Hangzhou Allsheng Instruments Co.,Ltd.). RT reactions were performed using 100 ng total RNA with the TaqMan miRNA RT kit (Applied Biosystems; Thermo Fisher Scientific, Inc., cat. no. 4366596) according to the manufacturer's instructions. qPCR reactions were conducted on a 7900 System (Applied Biosystems; Thermo Fisher Scientific, Inc.) using the Taq-Man miR-140 probe and gene-specific primers (Thermo Fisher Scientific, Inc., Assay ID 001187). Homo sapiens snRNA U6 qPCR Primer (Thermo Fisher Scientific, Inc., Assay ID 001973) were used as an internal control. qPCR was performed under the following

Table I. Primers used for reverse-transcription polymerase chain reaction.

Genes	Forward	Reverse
Aggrecan	TGAGCGGCAGCACTTTGAC	TGAGTACAGGAGGCTTGAGG
Col2a1	TCAGGAATTTGGTGTGGACATA	CCGGACTGTGAGGTTAGGATAG
Sox9	ATGAAGATGACCGACGAGCA	CAGTCGTAGCCTTTGAGCAC
GAPDH	GGCACAGTCAAGGCTGAGAATG	ATGGTGGTGAAGACGCCAGTA

conditions: 10 min at 95˚C, followed by 40 cycles of 95˚C for 10 sec, 20 sec at 60˚C and 10 sec at 72˚C.

Analysis of relative gene expression in cartilage cells. Cartilage cells subjected to IL-1β (10 ng/ml; R&D Systems, Inc.) and DPSC-derived exosome ($5x10^8$ particles/ml) treatment for 48 h were collected and total RNA was isolated using TRIzol reagent (Invitrogen, cat. no. 15596026) and reversed transcribed into first-strand cDNA using reverse transcriptase (Takara Bio, Inc.; cat. no. H2640A). RT-qPCR was performed using a SYBR-Green Master Mix (Takara Bio, Inc.; cat. no. RR820A) under the following conditions: 95˚C for 4 min, 40 cycles of 95˚C for 30 sec, 58˚C for 30 sec, 72˚C for 30 sec, followed by melting curve analysis of 95˚C for 30 sec, 72˚C for 30 sec, and 95˚C for 30 sec. Relative gene expression was calculated using the $2^{-\Delta\Delta Cq}$ (42) method and the data were normalized against *GAPDH*. The primers used are listed in Table I. Each PCR trial was performed in triplicate and repeated at least 3 times.

Animal experiments. Specific pathogen-free (SPF) male Sprague-Dawley (SD) rats (approximately 8 weeks old, weighing 200±20 g) were procured from the Shanghai SLAC Laboratory Animal Co., Ltd. [Certificate no. SCXK (Shanghai) 2017-0005] and maintained in the SPF laboratory of a local animal facility. The experimental protocol was approved by the local Medical Animal Experiment Ethics Committee of Zhejiang Provincial People's Hospital (no. 2019-034).

A total of 24 SD rats were randomly divided into the blank, OA model, exosome treatment and improved-exosome treatment groups, with 6 animals per group. Subsequently, 50 μl of 25 mg/ml iodoacetic acid (Sigma-Aldrich; Merck KGaA) was administered to the double knee joints to induce OA. The same amount of saline was administered into the knee joint cavities of the rats in the blank group. After 1 week, the exosome treatment group and improved-exosome treatment group were injected with 50 μl of exosomes ($5x10^{10}$ particles/ml, isolated from the culture supernatants of DPSCs as described above) and miR-140-enriched exosomes ($5x10^{10}$ particles/ml, isolated from the culture supernatants of miR140-transfacted DPSCs as described above), respectively, in the knee joint cavity of both hind limbs once a week; a total of 4 such injections were administered. The rats in the blank group and OA model group were administered the same amount of saline. The rats were sacrificed by an overdose of pentobarbital (150 mg/kg) intraperitoneally at 1 week after the end of treatment in accordance with a previous study (43).

Gross morphological analysis of the knee joints. At 1 week after the end of treatment, 3 rats were randomly selected from each group and anesthetized with 3% pentobarbital sodium (60 mg/kg) by intraperitoneal injection. An X-ray examination of the knee joint structure was then performed, and the grade of knee joint degradation of digital radiography films (PerkinElmer, Inc., CLS136341/F) was scored using a modified Kellgren-Lawrence scoring system for rats as previously described (44,45).

Histopathological examination of the knee joints. The rats were sacrificed, and their knee joints were isolated and fixed in 10% neutral-buffered formalin (Sangon Biotech) for 3 days and then decalcified for 2 weeks in buffered 12.5% EDTA (as previously described with some modifications) (46,47) and formalin solution. The tissues were then embedded in paraffin and were sliced along the longitudinal axis of the lower extremity at a thickness of 5 μm. They were subsequently stained with Safranin O-Fast Green (Sangon Biotech) and hematoxylin and eosin (H&E; Sangon Biotech). For Safranin O-Fast Green staining, sections were deparaffinized and stained with Safranin O for 5 min followed by Fast Green staining for 5 min at room temperature. For H&E staining, sections were deparaffinized and stained with hematoxylin staining solution for 10 min and then counterstained in eosin staining solution for 1 min at room temperature. The OARSI score was used to evaluate histological changes as previously described (48).

Primary isolation and culture of human chondrocytes. Normal human cartilage tissues were obtained from donation with written informed consent, and the protocol was approved by the Ethics Committee of Zhejiang Provincial People's Hospital in Hangzhou, China (2018 KY 012). Samples were obtained aseptically and digested using a standard protocol. Briefly, the tissues were cut into <1 mm^3 sections; they were then transferred to a culture flask, mixed with 5-fold volumes of 0.25% trypsin, and placed in a 37˚C, 5% CO_2 incubator for 30 min. The trypsin digestion solution was then discarded and 5-fold volumes of 0.05% type II collagenase (Sigma-Aldrich; Merck KGaA) were added to the tissue fragments. Subsequently, cells were collected every 4 h until the tissue block was digested. These chondrocytes were then cultured in DMEM supplemented with 20% FBS in a 37˚C, 5% CO_2 incubator.

Effects of DPSC-derived exosomes on IL-1β-treated chondrocytes in vitro. Normal human chondrocytes were treated with IL-1β to induce the inflammatory, *in vitro* model of OA as previously described with some modifications (49). The cells were divided into 4 different groups as follows: i) Normal culture;

ii) IL-1β (10 ng/ml, R&D Systems); iii) IL-1β (10 ng/ml) + DPSC-derived exosomes ($5x10^8$ particles/ml); and iv) IL-1β (10 ng/ml) + miR-140 enriched exosomes ($5x10^8$ particles/ml). Cells were collected for use in western blot analysis and apoptosis analysis at different time points.

Western blot analysis. Western blot analysis was performed as previously described (50). Briefly, exosomes or chondrocytes were added to cold lysis buffer (Beyotime Institute of Biotechnology, cat. no. P0013B) and incubated for 30 min on ice. The lysates were then centrifuged at 13,000 x g for 10 min at 4˚C. Subsequently, the supernatants were collected and quantified using the BCA protein assay kit (Beyotime Institute of Biotechnology, cat. no. P0011), and samples (20 μg) were separated on 10% polyacrylamide gels and transferred to Hybond-P membranes. 5% BSA (Beyotime Institute of Biotechnology, cat. no. ST025) was used for blocking at room temperature for 45 min prior to incubation with antibodies. The following antibodies were used: Rabbit anti-human CD63 (ProteinTech Group, Inc., cat. no. 25682-1-AP, at a dilution of 1:500), CD9 (ProteinTech Group, Inc., cat. no. 20597-1-AP at a dilution of 1:500) and Bcl-2 (ProteinTech Group, Inc., cat. no. 12789-1-AP at a dilution of 1:1,000), as well as rabbit anti-human Bax (Beyotime Institute of Biotechnology, cat. no. AF0057, at a dilution of 1:500) and Bad (Beyotime Institute of Biotechnology, cat. no. AF1009, at a dilution of 1:500). The primary antibodies were incubated at room temperature for 45 min. GAPDH (Beyotime Institute of Biotechnology, cat. no. AF1186, at a dilution of 1:2,000) served as the loading control. The blots were then incubated with HRP-conjugated goat anti-rabbit secondary antibody (Beyotime Institute of Biotechnology, cat. no. A0208, at a dilution of 1:1,000) for 45 min at room temperature and then processed for analysis using an ECL chemiluminescence kit (Beyotime Institute of Biotechnology). ImageJ (National Institutes of Health, v1.8.0) was further employed to analyze the grayscale values obtained by western blotting.

Apoptosis analysis. Apoptosis was determined using the Annexin V-propidium iodide (PI) binding assay as previously reported (51). The cells were harvested and labeled with Annexin V-FITC and PI for 15 min using a FITC Annexin V apoptosis detection kit I (BD Pharmingen). Apoptosis was evaluated using flow cytometry (Navios, Beckman Coulter, Inc.) within 30 min of staining, and the data were analyzed using FlowJo software v11.0. The extent of apoptosis was quantified as the percentage of Annexin V^+ cells. All experiments were performed in triplicate.

Statistical analysis. Data are presented as the means ± standard deviations of the results of at least 3 independent studies. Student's t-tests were utilized to identify differences among groups, as suitable. One-way ANOVA with the Bonferroni test was performed for multiple group comparisons. A P-value <0.05 was considered to indicate a statistical significant difference.

Results

Isolation and characterization of DPSCs. DPSCs were isolated from the pulp tissue of extracted human third molar teeth without caries, periodontal diseases, or infections. These cells are closely associated with MSCs found in the stromal compartment of various tissues, including the bone marrow. As shown in Fig. 1A, the cells exhibited a typical spindle-shaped morphology. DPSCs followed the criteria that defined multipotent MSCs, as recommended by the International Society for Cellular Therapy guidelines in 2006 (52). Following culture in a specific differentiation medium for 2-3 weeks, the isolated DPSCs successfully differentiated into mesenchymal derivatives, including osteoblasts (identified by Alizarin Red labeling), adipocytes (identified by Oil Red O labeling) and chondrocytes (identified by Alcian blue) (Fig. 1A). Furthermore, as revealed by flow cytometric assay, these cells were positively stained for the common MSC-associated markers, CD73, CD90 and CD105, and did not exhibit an expression of the hematopoietic markers, CD14, CD34 and HLA-DR (Fig. 1B).

Isolation and identification of exosomes from dental pulp stem cell lines. To examine the effects of miR-140-5p-transfected DPSCs on articular cartilage injuries, miR-140-5p mimic or negative control oligonucleotide were transfected into third-passage DPSCs via electroporation. The cells were collected 48 h later for total RNA extraction. RT-qPCR revealed that the cells transfected with the mimic exhibited a 10-fold increase in the miR-140-5p level compared with the negative control cells (Fig. 2A). Exosomes were collected from both types of DPSCs by centrifugation. Nanosight analysis indicated that the diameter of the majority of the DPSC-derived exosomes was approximately 134±29 nm (Fig. 2B). As shown in Fig. 2C, western blot analysis revealed that the DPSC-derived exosomes expressed exosomal markers, including CD9 and CD63. No significant differences in the expression levels of CD9 and CD63 between exosomes from the DPSCs with and without miR-140-5p transfection were observed ($P>0.05$). Finally, the results of RT-qPCR revealed a 4-fold increase in the miR-140-5p levels in exosomes derived from the miR-140-5p-overexpressing DPSCs than those from the control exosomes.

Effect of DPSC-derived exosomes on mRNA levels in chondrocytes. Subsequently, normal human chondrocytes were treated with IL-1β (10 ng/ml) with or without DPSC-derived exosomes. As shown in Fig. 3, IL-1β stimulation substantially decreased the chondrocyte ACAN, Col2α1 and Sox9 mRNA levels. However, the use of DPSC-derived exosomes elevated the corresponding mRNA levels, particularly the miR-140-5p-enriched exosomes.

DPSC-derived exosomes inhibit the IL-1β-induced apoptosis of chondrocytes. Chondrocytes from normal humans were treated with IL-1β (10 ng/ml) with or without DPSC-derived exosomes. The cells were trypsinized for apoptosis analysis at various time points. As shown in Fig. 4A and B, when exposed to IL-1β for 48 h, the DPSC-derived exosome groups (DPSC-derived exosomes and miR-140-5p-enriched exosomes) exhibited a decreased apoptosis compared with the control group (16.29±0.1% and 12.32±0.2% vs. 21.91±0.3% Annexin V^+ cells at 24 h; 24.91±0.1% and 18.14± 0.1% vs. 34.58±0.5% Annexin V^+ cells at 48 h; all $P<0.01$). The miR-140-5p-enriched exosome group exhibited a more

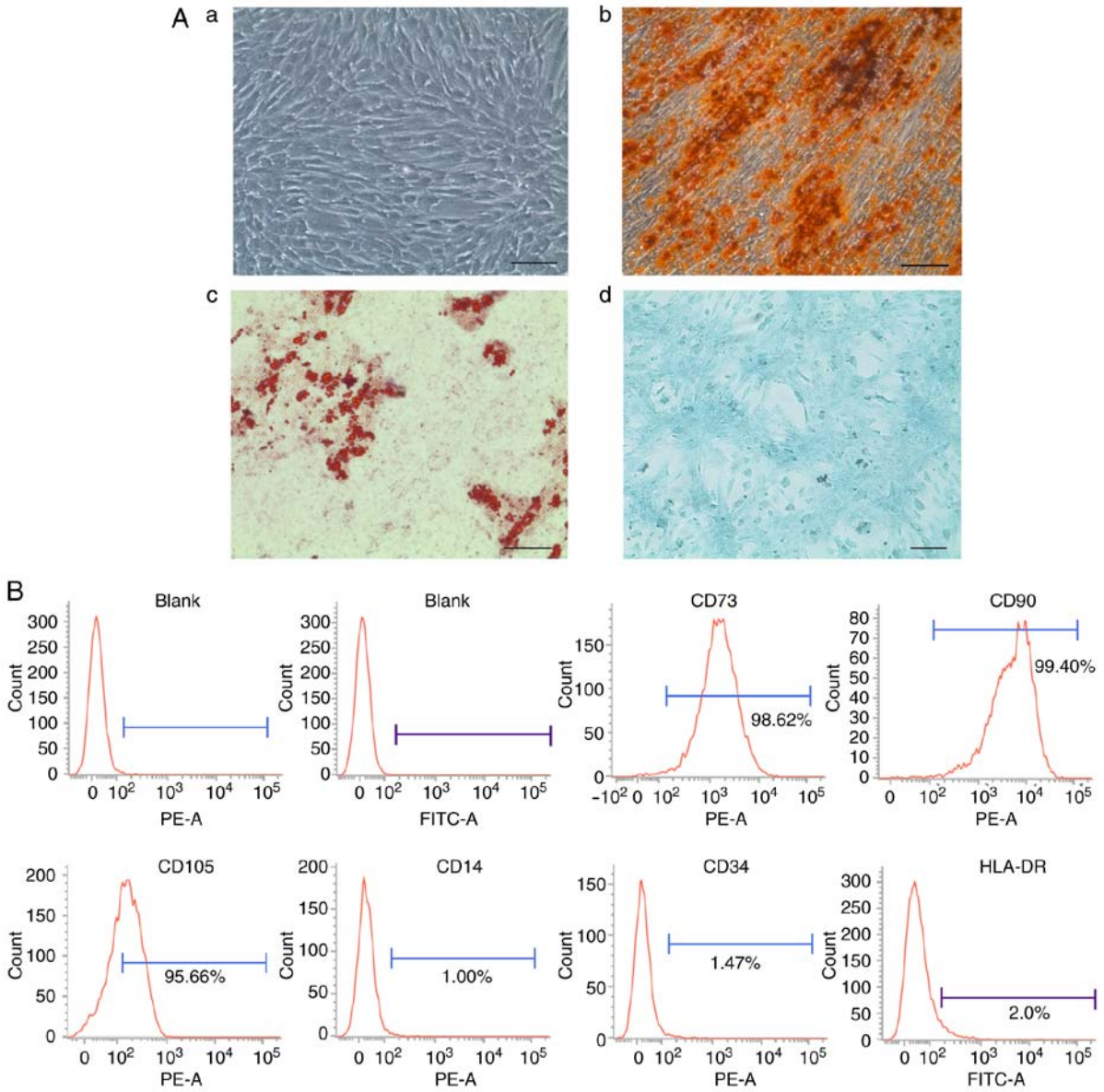

Figure 1. Characteristics of isolated DPSCs. (A-a) The morphology of third-passage DPSCs at 100% confluency. The culture medium was replaced with a specific-lineage induction medium. Inverted light microscopic image is shown representing DPSCs 2-3 weeks post-induction following staining with (A-b) Alizarin Red (red color represents mineralized nodules), (A-c) Oil Red O, and (A-d) Alcian blue. Scale bars, 50 μm. (B) The cell surface markers of isolated DPSCs were examined using flow cytometry. Similar to bone marrow-derived mesenchymal stem cells, DPSCs were positive for CD105, CD90 and CD73 and exhibited a weak or negative expression of the common hematopoietic markers, CD34, CD14, and HLA-DR. DPSCs, dental pulp stem cells.

significant reduction in cell apoptosis than the DPSC-derived exosome group (P<0.01) (Fig. 4A and B). Likewise, western blot analysis indicated a significant inhibition of the expression of apoptosis-related proteins in chondrocytes treated with miR-140-5p-enriched exosomes (Fig. 4C and D).

Influence of exosome treatments on knee joint X-ray scores in a rat model of OA. Subsequently, the rat model of OA was treated with the 2 above-mentioned types of DPSC-derived exosomes and then assessed using X-rays to determine the effects of the treatments (Fig. 5). In comparison with the sham-operated group, the OA model group exhibited evident stenosis, with visible osteophytes and osteosclerosis. This was in line with previous findings (53,54), indicating the generation of the rat model of OA was successfully established. Both DPSC-derived exosomes reduced the grade and severity of knee joint damage in rats with OA, as determined by X-ray score, improved the joint cavity structure, and reduced the formation of osteophytes, articular surface irregularity and osteosclerosis. Moreover, these effects were substantially enhanced following miR-140-5p-enriched exosome treatment.

Effect of exosome treatments on the pathology of the knee joint in rats with OA. To further assess the effects of exosome treatment on the knee condition in rats with OA, the histological sections of rat cartilage in all 4 groups were examined. As observed following Safranin O-Fast Green and H&E staining (Figs. 6A and S2A), the knee joint cartilage was uneven in the rat model OA group, and the thickness of the cartilage was reduced with visible apoptotic bodies. Furthermore, the lower edge of the cartilage was uneven, and pathological changes, including inflammatory cell

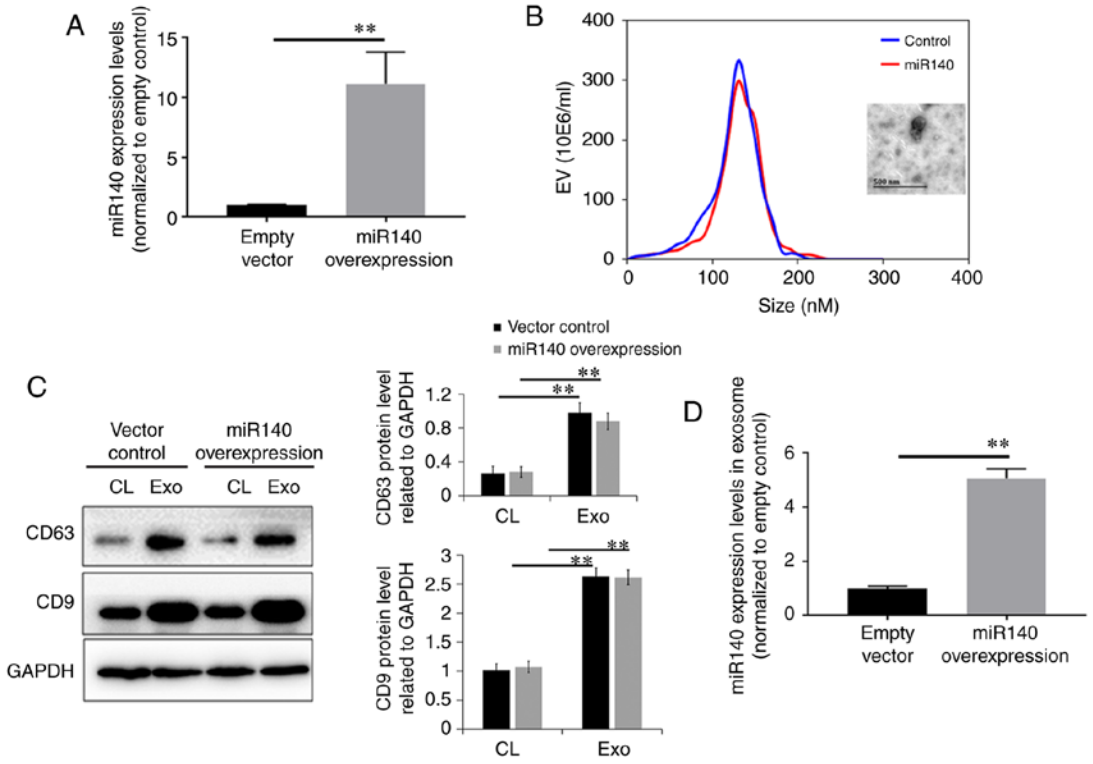

Figure 2. Characterization of DPSC-derived exosomes. (A) RT-qPCR findings indicated that cells transfected with mimic had around a 10-fold increase of miR-140-5p levels compared to the control. (B) The particle size distribution of exosomes measured by Nanosight. The insert is a representative TEM image of DPSC-derived exosomes. (C) Exosome surface markers measured by western blot analysis. (D) RT-qPCR findings revealed an increase of miR-140-5p levels in exosomes from miR-140-5p-overexpression of DPSCs compared with that of the control. **P<0.01 (means ± standard deviation, n=3). DPSCs, dental pulp stem cells; CL, cell lysates; Exo, exosomes.

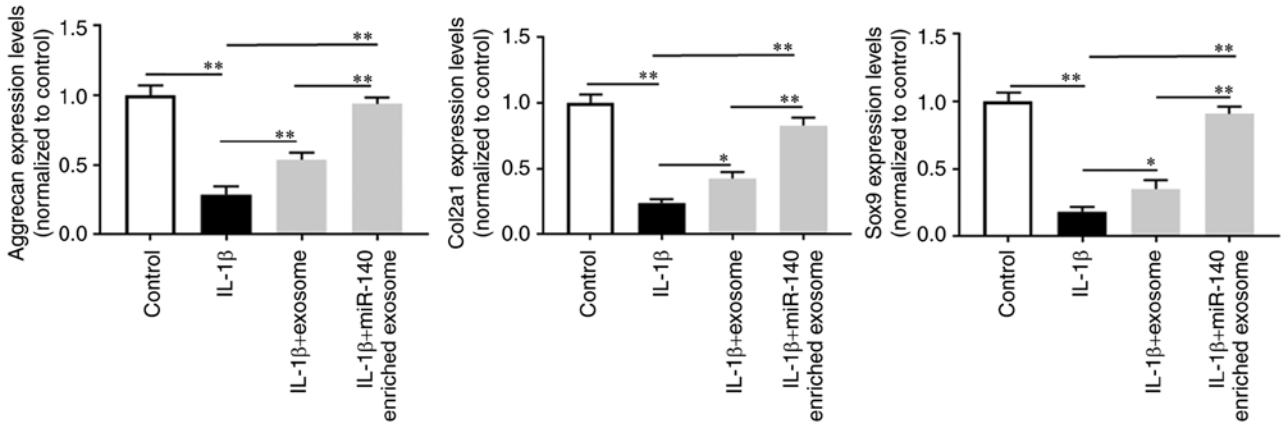

Figure 3. Effect of DPSC-derived exosomes on the expression of relative mRNA in normal chondrocytes. Chondrocytes from normal were induced by IL-1β (10 ng/ml) for 48 h, and the mRNA expression of aggrecan, Col2α1 and Sox9 was inhibited. Simultaneous administration of DPSC-derived exosomes substantially promoted the expression of these mRNAs. *P<0.05, **P<0.01 (means ± standard deviation, n=3). DPSCs, dental pulp stem cells.

infiltration, could be observed. The multiple administration of DPSC-derived exosomes improved the pathology of the rat knee joints to varying degrees, and the miR-140-5p-enriched exosomes substantially reduced the total pathological OARSI grading score (Figs. 6B and S2B).

Discussion

OA is a chronic degenerative process that is a common cause of disability in middle-aged and older adults. Its common clinical phenotypes include progressive cartilage deterioration, subchondral bone remodeling, loss of joint space, marginal osteophytosis, and loss of joint function, and it affects >80% of individuals aged of ≥55 years (55). The majority of patients with OA are treated with a combination of non-pharmacological (such as physiotherapy) and pharmacological treatments to reduce pain and inflammation. Although some patients exhibit temporary relief, the efficacy of these interventions is not consistent, and studies assessing the efficacy of these interventions are still being

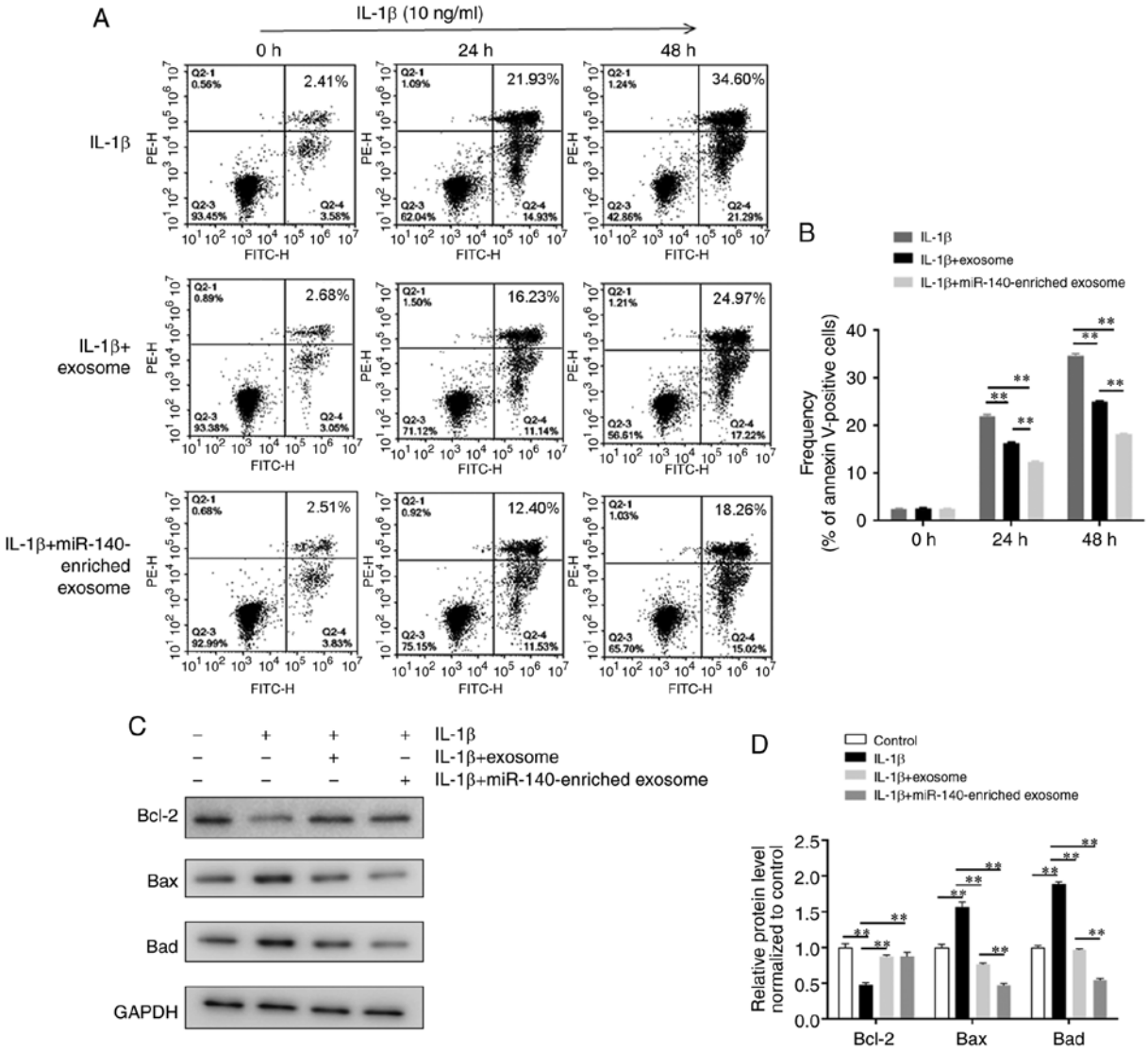

Figure 4. Effect of DPSCs-derived exosomes on IL-1β-induced apoptosis in normal chondrocytes. (A and B) Both types of DPSC-derived exosomes inhibited the response rates of chondrocytes to IL-1β treatment. miR-140-5p-enriched exosomes substantially enhanced the varying cell rates. (C and D) Western blot analyses indicated that the apoptosis-related protein expression in miR-140-5p-enriched exosome-treated chondrocytes was significantly inhibited following IL-1β treatment. **P<0.01 (means ± standard deviation, n=3). DPSCs, dental pulp stem cells.

conducted. In recent years, it has been proposed that MSCs improve chondrocyte regeneration and maintain articular cartilage in patients with OA (56).

MSCs are multipotent stromal cells that can differentiate into various cell types, including osteoblasts, adipocytes and chondrocytes (13-17). Apart from their ability to differentiate, the immune regulating function of MSC has received more attention in the past decades. Indeed, MSCs are used to treat various clinical conditions, particularly autoimmune diseases, including Crohn's disease, multiple sclerosis, lupus, COPD, Parkinson's and OA (32,57-60). However, these cells do not directly cure these conditions; the efficacy of MSC-based therapeutic strategies is ascribed more to paracrine secretion (61). MSCs influence the local microenvironment by secreting different bioactive factors. EVs are critical mediators of cell-to-cell communication in these situations. MSC-derived exosomes play a crucial role in regulating cell migration, proliferation, differentiation, and matrix synthesis. Moreover, MSC-derived exosomes have been shown to shuttle many bioactive components (proteins, lipids, mRNAs, miRNAs, lncRNAs, circRNAs and DNA) (31,62). Therefore, MSC exosomes may represent a new therapeutic alternative for OA. DPSCs are type of MSCs derived from dental pulp, which have become one of the best cells for periodontal tissue engineering owing to their excellent growth and differentiation capacity in *ex vivo* cultures (63,64). Reportedly, cultured DPSCs have a pale, round, or oval central nucleus with multiple nucleoli, showing active DNA transcription, and RNA synthesis. Numerous cytoplasmic vacuoles also show exuberant cellular secretory vesicles (65).

Consistent with previously published data, the current study proposed that miR-140 plays a role in chondrogenesis. miR-140 has been reported to play essential roles in regulating cartilage homeostasis and development by enhancing the expression of SOX9 and ACAN (37-39). In addition, miR-140-5p can regulate the proliferation and differentiation of DPSC and inhibit the differentiation of DPSCs into odontoblastic cells (66,67). In the present study, miR-140-5p was first overexpressed in DPSCs

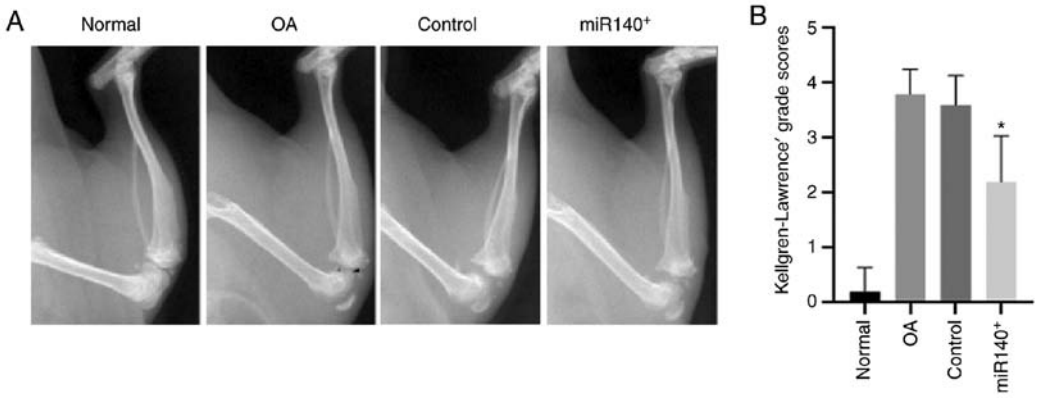

Figure 5. Effects of exosome on joints in rats determined by X-ray. (A) In comparison with the blank control groups, articular cavity stenosis was found in the other 3 OA model groups, including visible osteophytes and osteosclerosis. The administration of DPSC-derived exosomes can improve the structure of the articular cavity and reduce osteophyte formation. Black arrow indicates the formation of osteophytes; the red asterisk indicates the irregularity of the articular surface. (B) X-ray images were scored using Kellgren-Lawrence's grades. In comparison with the model group, administration of miR-140-5p-enriched exosomes substantially reduced the knee joint X-ray scores and the grade of 'severe' (grade 4 to grade 2) ($^{*}P<0.05$; means ± standard deviation, n=3). DPSCs, dental pulp stem cells; OA, osteoarthritis.

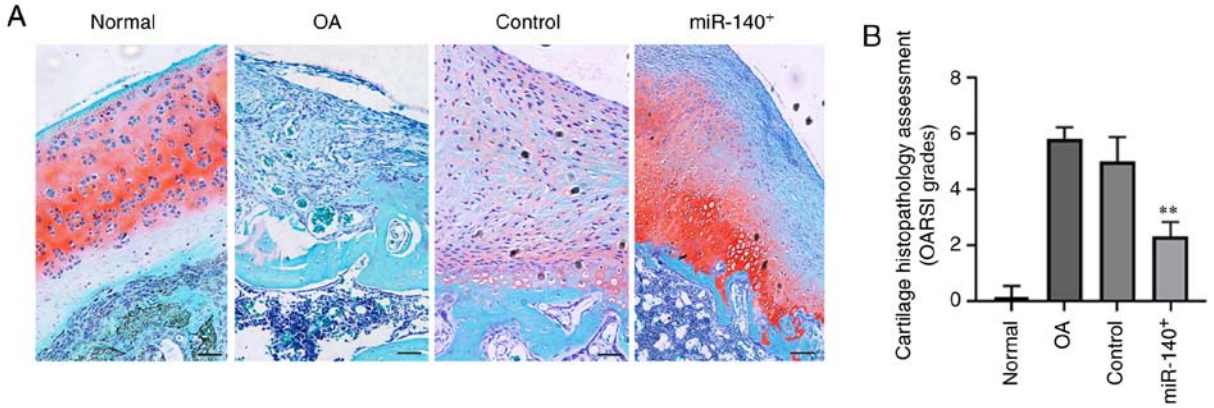

Figure 6. Effect of DPSC-derived exosomes on cartilage tissue in rats with OA. (A) The histological sections of rat cartilage tissues were stained using Safranin O-Fast Green. The photomicrograph showed a loss of surface layers in OA rats compared to the sham operation group (blank control group). Changes in the ground substance can also be observed. Treatments with DPSC-derived exosomes could improve the pathology changes in OA rats. (B) Photomicrograph of Safranin O-Fast Green staining was scored using the OARSI score system ($^{**}P<0.01$; means ± standard deviation, n=6). Scale bars, 50 μm. DPSCs, dental pulp stem cells; OA, osteoarthritis.

and the increased burden of miR-140-5p in exosomes isolated from DPSC culture supernatant was validated. The data indicated that DPSC-derived exosomes promoted the expression of chondrocyte-related mRNAs, including AGAN, Col2α1 and Sox9, in cultured normal human chondrocytes. Sox9 is the master regulator of a transcription factor for chondrogenesis. In particular, it has been shown to activate Col11A1, Col2A1 and ACAN, all of which play pivotal functions during chondrogenesis. Col11A1 has been proven to be essential in cartilage architecture during chondrogenesis by modulating chondrocyte behavior (68). ACAN can improve chondrogenesis by delaying hypertrophic chondrocyte maturation (69). Additionally, the effect of DPSC-derived exosomes on the expression of chondrocyte-related mRNAs was substantially enhanced by miR-140-5p enriched exosomes. The findings from Annexin V-PI flow cytometry and western blot analysis suggested that the miR-140-5p-enriched exosomes significantly inhibited the IL-1β-induced apoptosis of primary cultured human chondrocytes. Furthermore, the effects of DPSC-derived exosomes were explored in a rat model of OA, and the results were consistent with the *in vitro* findings.

In conclusion, the findings presented herein demonstrate that the overexpression of exosomal-miR-140-5p substantially attenuates OA both *in vitro* and *in vivo*. Although previous stem cell-related studies (70,71) have also indicated a protective effect of stem cell-derived exosomes in models of OA, the present study determined that exosomes from miR140-overexpressing DPSCs relieved symptoms of OA by inhibiting the apoptosis of chondrocytes and promoting cartilage repair. Hence, the present study provides a more efficient, safer and stem cell-independent strategy for the treatment of OA. To the best of our knowledge, this is the first study to adopt genetically modified DPSCs to produce miRNA-140-enriched exosomes for the treatment of OA. Nonetheless, further studies are required to clarify the specific function of exosomal-miR-140-5p in models of OA prior to the clinical application of exosome-based therapy in OA.

Acknowledgements

Not applicable.

Funding

The present study was supported by the Social Development Project of Public Welfare Technology Application in Zhejiang Province (grant no. LGF18H060007), and the Key Technologies R&D Program of Zhejiang Province (grant no. 2019C03041).

Availability of data and materials

All data generated or analyzed in the current study are included in this published article or relevant supplementary material, or are available from the corresponding author upon reasonable request.

Authors' contributions

TL participated in the study design. NW performed the experiments. LW and RZ analyzed the data. YFC contributed to the study design and data acquisition, and provided valuable advice and drafted the manuscript. RP supervised the study, performed the experiments and revised the manuscript. All authors read and approved the final manuscript.

Ethics approval and consent to participate

The Ethics Committee of S-Evans Biosciences approved the collection of human samples (no. 2020-01). The Ethics Committee of Zhejiang Provincial People's Hospital approved the experiments using human cartilage (2018 KY 012). All patients provided written informed consent. The experimental protocol was approved by the local Medical Animal Experiment Ethics Committee of Zhejiang Provincial People's Hospital (no. 2019-034).

Patient consent for publication

Not applicable.

Competing interests

The authors declare that there are no competing interests. The company 'S-Evans Biosciences', with which RP is affiliated, had no role in the study design or outcomes.

References

1. Bhosale AM and Richardson JB: Articular cartilage: Structure, injuries and review of management. Br Med Bull 87: 77-95, 2008.
2. Buckwalter JA, Anderson DD, Brown TD, Tochigi Y and Martin JA: The roles of mechanical stresses in the pathogenesis of osteoarthritis: Implications for treatment of joint injuries. Cartilage 4: 286-294, 2013.
3. Dieppe PA and Lohmander LS: Pathogenesis and management of pain in osteoarthritis. Lancet 365: 965-973, 2005.
4. Van Osch GJ, Brittberg M, Dennis JE, Bastiaansen-Jenniskens YM, Erben RG, Konttinen YT and Luyten FP: Cartilage repair: Past and future-lessons for regenerative medicine. J Cell Mol Med 13: 792-810, 2009.
5. Sgaglione NA, Miniaci A, Gillogly SD and Carter TR: Update on advanced surgical techniques in the treatment of traumatic focal articular cartilage lesions in the knee. Arthroscopy 18 (Suppl 1): S9-S32, 2002.
6. Temenoff JS and Mikos AG: Review: Tissue engineering for regeneration of articular cartilage. Biomaterials 21: 431-440, 2000.
7. Simon TM and Jackson DW: Articular cartilage: Injury pathways and treatment options. Sports Med Arthrosc Rev 26: 31-39, 2018.
8. Phinney DG and Prockop DJ: Concise review: Mesenchymal stem/multipotent stromal cells: The state of transdifferentiation and modes of tissue repair-current views. Stem Cells 25: 2896-2902, 2007.
9. Park D, Spencer JA, Koh BI, Kobayashi T, Fujisaki J, Clemens TL, Lin CP, Kronenberg HM and Scadden DT: Endogenous bone marrow MSCs are dynamic, fate-restricted participants in bone maintenance and regeneration. Cell Stem Cell 10: 259-272, 2012.
10. Zuk PA, Zhu M, Ashjian P, De Ugarte DA, Huang JI, Mizuno H, Alfonso ZC, Fraser JK, Benhaim P and Hedrick MH: Human adipose tissue is a source of multipotent stem cells. Mol Biol Cell 13: 4279-4295, 2002.
11. Qiao C, Xu W, Zhu W, Hu J, Qian H, Yin Q, Jiang R, Yan Y, Mao F, Yang H, *et al*: Human mesenchymal stem cells isolated from the umbilical cord. Cell Biol Int 32: 8-15, 2008.
12. Valtieri M and Sorrentino A: The mesenchymal stromal cell contribution to homeostasis. J Cell Physiol 217: 296-300, 2008.
13. Romanov YA, Darevskaya AN, Merzlikina NV and Buravkova LB: Mesenchymal stem cells from human bone marrow and adipose tissue: Isolation, characterization, and differentiation potentialities. Bull Exp Biol Med 140: 138-143, 2005.
14. Timper K, Seboek D, Eberhardt M, Linscheid P, Christ-Crain M, Keller U, Müller B and Zulewski H: Human adipose tissue-derived mesenchymal stem cells differentiate into insulin, somatostatin, and glucagon expressing cells. Biochem Biophys Res Commun 341: 1135-1140, 2006.
15. Sonomoto K, Yamaoka K, Oshita K, Fukuyo S, Zhang X, Nakano K, Okada Y and Tanaka Y: Interleukin-1β induces differentiation of human mesenchymal stem cells into osteoblasts via the Wnt-5a/receptor tyrosine kinase-like orphan receptor 2 pathway. Arthritis Rheum 64: 3355-3363, 2012.
16. Liu ZJ, Zhuge Y and Velazquez OC: Trafficking and differentiation of mesenchymal stem cells. J Cell Biochem 106: 984-991, 2009.
17. Yu DA, Han J and Kim BS: Stimulation of chondrogenic differentiation of mesenchymal stem cells. Int J Stem Cells 5: 16-22, 2012.
18. Caplan AI: MSCs: The sentinel and safe-guards of injury. J Cell Physiol 231: 1413-1416, 2016.
19. Anton K, Banerjee D and Glod J: Macrophage-associated mesenchymal stem cells assume an activated, migratory, pro-inflammatory phenotype with increased IL-6 and CXCL10 secretion. PLoS One 7: e35036, 2012.
20. Di Gh, Liu Y, Lu Y, Liu J, Wu C and Duan HF: IL-6 secreted from senescent mesenchymal stem cells promotes proliferation and migration of breast cancer cells. PLoS One 9: e113572, 2014.
21. Qu X, Liu X, Cheng K, Yang R and Zhao RC: Mesenchymal stem cells inhibit Th17 cell differentiation by IL-10 secretion. Exp Hematol 40: 761-770, 2012.
22. Noh MY, Lim SM, Oh KW, Cho KA, Park J, Kim KS, Lee SJ, Kwon MS and Kim SH: Mesenchymal stem cells modulate the functional properties of microglia via TGF-beta secretion. Stem Cells Transl Med 5: 1538-1549, 2016.
23. Mias C, Lairez O, Trouche E, Roncalli J, Calise D, Seguelas MH, Ordener C, Piercecchi-Marti MD, Auge N, Salvayre AN, *et al*: Mesenchymal stem cells promote matrix metalloproteinase secretion by cardiac fibroblasts and reduce cardiac ventricular fibrosis after myocardial infarction. Stem Cells 27: 2734-2743, 2009.
24. Lozito TP and Tuan RS: Mesenchymal stem cells inhibit both endogenous and exogenous MMPs via secreted TIMPs. J Cell Physiol 226: 385-396, 2011.
25. Rani S, Ryan AE, Griffin MD and Ritter T: Mesenchymal stem cell-derived extracellular vesicles: Toward cell-free therapeutic applications. Mol Ther 23: 812-823, 2015.
26. Lo Sicco C, Reverberi D, Balbi C, Ulivi V, Principi E, Pascucci L, Becherini P, Bosco MC, Varesio L, Franzin C, *et al*: Mesenchymal stem cell-derived extracellular vesicles as mediators of anti-inflammatory effects: Endorsement of macrophage polarization. Stem Cells Transl Med 6: 1018-1028, 2017.
27. Raposo G and Stoorvogel W: Extracellular vesicles: Exosomes, microvesicles, and friends. J Cell Biol 200: 373-383, 2013.
28. Théry C, Zitvogel L and Amigorena S: Exosomes: Composition, biogenesis and function. Nat Rev Immunol 2: 569-579, 2002.
29. Bang OY and Kim EH: Mesenchymal stem cell-derived extracellular vesicle therapy for stroke: Challenges and progress. Front Neurol 10: 211, 2019.
30. Zhang ZG, Buller B and Chopp M: Exosomes-beyond stem cells for restorative therapy in stroke and neurological injury. Nat Rev Neurol 15: 193-203, 2019.

31. Yu B, Zhang X and Li X: Exosomes derived from mesenchymal stem cells. Int J Mol Sci 15: 4142-4157, 2014.
32. Cosenza S, Ruiz M, Toupet K, Jorgensen C and Noël D: Mesenchymal stem cells derived exosomes and microparticles protect cartilage and bone from degradation in osteoarthritis. Sci Rep 7: 16214, 2017.
33. Liu Y, Lin L, Zou R, Wen C, Wang Z and Lin F: MSC-derived exosomes promote proliferation and inhibit apoptosis of chondrocytes via lncRNA-KLF3-AS1/miR-206/GIT1 axis in osteoarthritis. Cell Cycle 17: 2411-2422, 2018.
34. Dong S, Yang B, Guo H and Kang F: MicroRNAs regulate osteogenesis and chondrogenesis. Biochem Biophys Res Commun 418: 587-591, 2012.
35. Shang J, Liu H and Zhou Y: Roles of micro RNA s in prenatal chondrogenesis, postnatal chondrogenesis and cartilage-related diseases. J Cell Mol Med 17: 1515-1524, 2013.
36. Liu H, Sun Q, Wan C, Li L, Zhang L and Chen Z: MicroRNA-338-3p regulates osteogenic differentiation of mouse bone marrow stromal stem cells by targeting Runx2 and Fgfr2. J Cell Physiol 229: 1494-1502, 2014.
37. Miyaki S, Sato T, Inoue A, Otsuki S, Ito Y, Yokoyama S, Kato Y, Takemoto F, Nakasa T, Yamashita S, *et al*: MicroRNA-140 plays dual roles in both cartilage development and homeostasis. Genes Dev 24: 1173-1185, 2010.
38. Buechli ME, Lamarre J and Koch TG: MicroRNA-140 expression during chondrogenic differentiation of equine cord blood-derived mesenchymal stromal cells. Stem Cells Dev 22: 1288-1296, 2013.
39. Karlsen TA, Jakobsen RB, Mikkelsen TS and Brinchmann JE: microRNA-140 targets RALA and regulates chondrogenic differentiation of human mesenchymal stem cells by translational enhancement of SOX9 and ACAN. Stem Cells Dev 23: 290-304, 2014.
40. Hilkens P, Gervois P, Fanton Y, Vanormelingen J, Martens W, Struys T, Politis C, Lambrichts I and Bronckaers A: Effect of isolation methodology on stem cell properties and multilineage differentiation potential of human dental pulp stem cells. Cell Tissue Res 353: 65-78, 2013.
41. Greening DW, Xu R, Ji H, Tauro BJ and Simpson RJ: A protocol for exosome isolation and characterization: Evaluation of ultracentrifugation, density-gradient separation, and immunoaffinity capture methods. Methods Mol Biol 1295: 179-209, 2015.
42. Livak KJ and Schmittgen TD: Analysis of relative gene expression data using real-time quantitative PCR and the 2(-Delta Delta C(T)) method. Methods 25: 402-408, 2001.
43. Yan L, Zhou L, Xie D, Du W, Chen F, Yuan Q, Tong P, Shan L and Efferth T: Chondroprotective effects of platelet lysate towards monoiodoacetate-induced arthritis by suppression of TNF-α-induced activation of NF-KB pathway in chondrocytes. Aging (Albany NY) 11: 2797-2811, 2019.
44. Jay GD, Elsaid KA, Kelly KA, Anderson SC, Zhang L, Teeple E, Waller K and Fleming BC: Prevention of cartilage degeneration and gait asymmetry by lubricin tribosupplementation in the rat following anterior cruciate ligament transection. Arthritis Rheum 64: 1162-1171, 2012.
45. Teeple E, Elsaid KA, Jay GD, Zhang L, Badger GJ, Akelman M, Bliss TF and Fleming BC: Effects of supplemental intra-articular lubricin and hyaluronic acid on the progression of posttraumatic arthritis in the anterior cruciate ligament-deficient rat knee. Am J Sports Med 39: 164-172, 2011.
46. Gao X, Jiang S, Du Z, Ke A, Liang Q and Li X: KLF2 protects against osteoarthritis by repressing oxidative response through activation of Nrf2/ARE signaling in vitro and in vivo. Oxid Med Cell Longev 2019: 8564681, 2019.
47. Inomata K, Tsuji K, Onuma H, Hoshino T, Udo M, Akiyama M, Nakagawa Y, Katagiri H, Miyatake K, Sekiya I, *et al*: Time course analyses of structural changes in the infrapatellar fat pad and synovial membrane during inflammation-induced persistent pain development in rat knee joint. BMC Musculoskelet Disord 20: 8, 2019.
48. Pritzker KP, Gay S, Jimenez SA, Ostergaard K, Pelletier JP, Revell PA, Salter D and van den Berg WB: Osteoarthritis cartilage histopathology: Grading and staging. Osteoarthritis Cartilage 14: 13-29, 2006.
49. Castro Martins M, Peffers MJ, Lee K and Rubio-Martinez LM: Effects of stanozolol on normal and IL-1β-stimulated equine chondrocytes in vitro. BMC Vet Res 14: 103, 2018.
50. Fang QX, Zheng XC and Zhao HJ: L1CAM is involved in lymph node metastasis via ERK1/2 signaling in colorectal cancer. Am J Transl Res 12: 837-846, 2020.
51. Crowley LC, Marfell BJ, Scott AP and Waterhouse NJ: Quantitation of apoptosis and necrosis by Annexin V binding, propidium iodide uptake, and flow cytometry. Cold Spring Harb Protoc 2016: 2016.
52. Dominici M, Le Blanc K, Mueller I, Slaper-Cortenbach I, Marini F, Krause D, Deans R, Keating A, Prockop DJ and Horwitz E: Minimal criteria for defining multipotent mesenchymal stromal cells. The international society for cellular therapy position statement. Cytotherapy 8: 315-317, 2006.
53. Kellgren JH and Lawrence JS: Radiological assessment of osteo-arthrosis. Ann Rheum Dis 16: 494-502, 1957.
54. Kohn MD, Sassoon AA and Fernando ND: Classifications in brief: Kellgren-lawrence classification of osteoarthritis. Clin Orthop Relat Res 474: 1886-1893, 2016.
55. Loeser RF, Goldring SR, Scanzello CR and Goldring MB: Osteoarthritis: A disease of the joint as an organ. Arthritis Rheum 64: 1697-1707, 2012.
56. Qi Y, Feng G and Yan W: Mesenchymal stem cell-based treatment for cartilage defects in osteoarthritis. Mol Biol Rep 39: 5683-5689, 2012.
57. Voswinkel J, Francois S, Simon JM, Benderitter M, Gorin NC, Mohty M, Fouillard L and Chapel A: Use of mesenchymal stem cells (MSC) in chronic inflammatory fistulizing and fibrotic diseases: A comprehensive review. Clin Rev Allergy Immunol 45: 180-192, 2013.
58. Bai L, Lennon DP, Caplan AI, DeChant A, Hecker J, Kranso J, Zaremba A and Miller RH: Hepatocyte growth factor mediates mesenchymal stem cell-induced recovery in multiple sclerosis models. Nat Neurosci 15: 862-870, 2012.
59. Liu S, Liu D, Chen C, Hamamura K, Moshaverinia A, Yang R, Liu Y, Jin Y and Shi S: MSC transplantation improves osteopenia via epigenetic regulation of notch signaling in lupus. Cell Metab 22: 606-618, 2015.
60. Gu W, Song L, Li XM, Wang D, Guo XJ and Xu WG: Mesenchymal stem cells alleviate airway inflammation and emphysema in COPD through down-regulation of cyclooxygenase-2 via p38 and ERK MAPK pathways. Sci Rep 5: 1-11, 2015.
61. Lee JW, Fang X, Krasnodembskaya A, Howard JP and Matthay MA: Concise review: Mesenchymal stem cells for acute lung injury: Role of paracrine soluble factors. Stem Cells 29: 913-919, 2011.
62. Deng H, Sun C, Sun Y, Li H, Yang L, Wu D, Gao Q and Jiang X: Lipid, protein, and microRNA composition within mesenchymal stem cell-derived exosomes. Cell Reprogram 20: 178-186, 2018.
63. Ashri NY, Ajlan SA and Aldahmash AM: Dental pulp stem cells: Biology and use for periodontal tissue engineering. Saudi Med J 36: 1391-1399, 2015.
64. Graziano A, d'Aquino R, Laino G and Papaccio G: Dental pulp stem cells: A promising tool for bone regeneration. Stem Cell Rev 4: 21-26, 2008.
65. Merckx G, Hosseinkhani B, Kuypers S, Vanspringel L, Irobi J, Michiels L, Lambrichts I and Bronckaers A: Extracellular vesicles from human dental pulp stem cells as proangiogenic strategy in tooth regeneration. J Extracellular Vesicles 7: 134-134, 2018.
66. Lu X, Chen X, Xing J, Lian M, Huang D, Lu Y, Feng G and Feng X: miR-140-5p regulates the odontoblastic differentiation of dental pulp stem cells via the Wnt1/β-catenin signaling pathway. Stem Cell Res Ther 10: 226, 2019.
67. Sun DG, Xin BC, Wu D, Zhou L, Wu HB, Gong W and Lv J: miR-140-5p-mediated regulation of the proliferation and differentiation of human dental pulp stem cells occurs through the lipopolysaccharide/toll-like receptor 4 signaling pathway. Eur J Oral Sci 125: 419-425, 2017.
68. Li A, Wei Y, Hung C and Vunjak-Novakovic G: Chondrogenic properties of collagen type XI, a component of cartilage extracellular matrix. Biomaterials 173: 47-57, 2018.
69. Caron MMJ, Janssen MPF, Peeters L, Haudenschild DR, Cremers A, Surtel DAM, van Rhijn LW, Emans PJ and Welting TJM: Aggrecan and COMP improve periosteal chondrogenesis by delaying chondrocyte hypertrophic maturation. Front Bioeng Biotechnol 8: 1036, 2020.
70. Mianehsaz E, Mirzaei HR, Mahjoubin-Tehran M, Rezaee A, Sahebnasagh R, Pourhanifeh MH, Mirzaei H and Hamblin MR: Mesenchymal stem cell-derived exosomes: A new therapeutic approach to osteoarthritis? Stem Cell Res Ther 10: 340, 2019.
71. Zhu Y, Wang Y, Zhao B, Niu X, Hu B, Li Q, Zhang J, Ding J, Chen Y and Wang Y: Comparison of exosomes secreted by induced pluripotent stem cell-derived mesenchymal stem cells and synovial membrane-derived mesenchymal stem cells for the treatment of osteoarthritis. Stem Cell Res Ther 8: 64, 2017.